

INTERACTION OF LASER RADIATION WITH MATTER https://doi.org/10.1070/QEL16790

Ablation of hexagonal boron nitride by UV laser radiation

V.V. Kononenko, M.S. Komlenok, M.A. Dezhkina, V.M. Gololobov, V.I. Konov

Abstract. **We report an experimental study of ablation of hexagonal boron nitride ceramics irradiated by 193- and 248-nm laser pulses. The dependences of the material removal rate and the crater wall slope on the energy density in the irradiation spot are obtained. An ablation regime is found, when the material removal rate reaches 5 μm per pulse, which is not typical of nanosecond laser radiation. It is shown that at relatively low radiation intensities (about 5–10 J cm^{-2}), the slope angle of the formed crater wall does not exceed 20°.**

Keywords: *refractive optics, X-ray, UV laser radiation, laser ablation, boron nitride, ceramics.*

1. Introduction

Recently, boron nitride (BN) has been studied very closely, which is associated with broad prospects for its use in optics and electronics. Boron nitride is a wide-gap semiconductor, has high thermal conductivity, chemical and temperature stability, extreme mechanical hardness, and high melting point. Boron nitride is iso-electronic to carbon and, like it, exists in several allotropic modifications, as well as in amorphous form. The most common and easily synthesised crystalline form of boron nitride is hexagonal boron nitride (h-BN), which has a graphite-like structure. However, with the use of h-BN, the existing epitaxial growth technologies of large substrates of high crystalline quality, which are necessary for the practical use of boron nitride in real devices, are still far from perfect. Boron nitride is currently available mainly in the form of ceramics. Difficulties in micro/nano surface treatment of BN substrates are also a significant deterrent to the wide use of this material.

Despite these problems, the unique properties of boron nitride stimulate the study of its properties and new ways of application. For example, of special attention is the production of single-photon emitters in single-layer and multilayer h-BN films, which can work effectively at room temperature, thus opening up new possibilities in the design of photon structures [1–3]. Considerable efforts are directed to the synthesis and study of hexagonal nanotubes [4] and monolayers [5].

Interest in laser processing of boron nitride is due to the prospect of its use as a material for refractive optics of the X-ray range (1–100 keV) [6]. It is known that the lower the ratio of the X-ray absorption coefficient for a given material to its density, the more efficient the lens of this material will work [7]. Since this ratio is in the first approximation proportional to $Z^3/(\hbar\omega^3)$ (Z is the atomic number of the element, and $\hbar\omega$ is the photon energy), only light elements are suitable for this purpose. Traditionally, refractive X-ray lenses are fabricated from beryllium and aluminium [7]; nevertheless, synthetic diamond is gradually increasing in use [8]. In this case, boron nitride can be competitive with them, but to do this, the above problems of synthesising and processing BN substrates must be solved.

Requirements to the processing of a substrate in the manufacture of X-ray lenses are governed by its design, which, in turn, is determined by the optical properties of the solid in the X-ray range. The refractive index n of the medium in this region of the spectrum is less than unity; therefore, the simplest focusing element is a concave spherical lens. Since the X-ray refraction is very small ($n \approx 1-10^{-6}$), in order to obtain a noticeable focusing effect, a set of lenses is produced, one after the other along the optical axis [6]. Such a focusing element is a set of cylindrical holes drilled along one line in a plane-parallel plate. When X-rays propagate along this line, the element works as a cylindrical lens.

In this paper, we investigate the possibility of using laser ablation for perforation of h-BN ceramics. It should be noted that the study of the features of the intense radiation–boron nitride interaction was mainly focused on the problems of laser deposition [9, 10], including research on the laser torch [11], mutual transformation of its allotropes [12], synthesis of nanostructures [4, 13, 14] and photosimulation of the surface [3, 15, 16]. At the same time, data on laser microprocessing and profiling of BN targets are of rather limited, often qualitative character [17]. Today, ablation by a nanosecond CO_2 laser (λ = 9–10.6 μm) [18], a picosecond Nd:YAG laser (λ = 1064 nm) [19] and a femtosecond Ti:sapphire laser (λ = 790 nm) [20] is studied well. In the first case, the transfer of pulse energy occurs due to lattice absorption, and in the second and third cases it is due to nonlinear absorption. We failed to find data on ablation of boron nitride by nanosecond UV radiation, which should be most effective from the point of view of drilling and cutting of thick plates. In this paper, we bridge this gap and describe the results of ablation of the h-BN surface by using UV radiation from an excimer laser.

V.V. Kononenko, M.S. Komlenok, M.A. Dezhkina, V.I. Konov A.M. Prokhorov General Physics Institute, Russian Academy of Sciences, ul. Vavilova 38, 119991 Moscow, Russia; National Research Nuclear University 'MEPhI', Kashirskoe sh. 31, 115409 Moscow, Russia; e-mail: vitali.kononenko@gmail.com;
V.M. Gololobov A.M. Prokhorov General Physics Institute, Russian Academy of Sciences, ul. Vavilova 38, 119991 Moscow, Russia

Received 27 July 2018; revision received 17 September 2018
Kvantovaya Elektronika **48** (11) 996–999 (2018)
Translated by I.A. Ulitkin

2. Experiment

In the experiments, we used h-BN ceramic tablets sintered at a temperature of 200 °C and a pressure of 0.6 GPa. The thickness of the tablets was 2 mm; the surface roughness was ~2 μm.

The target surface was subjected to UV radiation from an excimer laser (CL7100 model, Physics Instrumentation Centre, A.M. Prokhorov General Physics Institute, Russian Academy of Sciences), emitting nanosecond pulses (λ = 15 ns). The laser wavelength was determined by the composition of the working mixture: 248 nm for the KrF mixture and 193 nm for the ArF mixture. The laser pulse energy reached 400 mJ at a pulse repetition rate of up to 100 Hz. In the experiments described, the laser served as a radiation source in a projection optical system, uniformly illuminating a square mask. Then the mask image demagnified by a factor of 20 was projected onto the sample surface with a short-focus lens having a numerical aperture NA = 0.15. Since UV radiation experiences significant absorption in the air [21], the laser energy was measured directly in front of the sample. The size of the laser spot was 100–200 μm. In this case, the local energy density on the sample surface was constant within the irradiation spot and reached ~30 J cm^{-2}. The experiments were carried out by varying the energy density in the range from 0.1 to 30 J cm^{-2} and the number of laser pulses from 1 to 200000.

Optical as well as scanning electron microscopy was used to analyse the surface after laser irradiation. Measurements of the surface etching depth were carried out using 50$^{\times}$ and 100$^{\times}$ lenses. The data presented below took into account only relatively deep craters, over 10 μm. Each measurement was repeated several times to minimise errors. The total measurement error of the crater depth was about 2 μm (20% for small craters).

3. Results and discussion

The advantages of nanosecond laser pulses are the high material removal rate and the energy efficiency of the process. The disadvantages (in particular, for metals) include the low quality of processing, which is mainly due to the material melting in the impact zone and the complex hydrodynamics of the melt during its cooling and recrystallisation. In our experiments, no trace of the melt on the surface of boron nitride was found either in the ablation zone or in its vicinity. This observation is consistent with the results of other works that either indicate the absence of melting or do not confirm its presence for a wide range of irradiation intensities and durations [18, 20].

Figure 1 shows the dependences of the ablation crater depth on the number of irradiation pulses at a wavelength of 248 nm. One can see that at relatively low energy densities (F ~ 10 J cm^{-2}) the ablation rate reaches several micrometers per pulse. As far as we know, such extreme ablation rates of boron nitride have been observed for the first time. In previous works with energy densities of 10–100 J cm^{-2}, the maximum ablation rates were less than 0.5 μm per pulse [18, 20]. Note that the material removal rate begins to fall when the crater reaches a depth of approximately 50–60 μm, which is apparently due to the gradual development of roughness at its bottom (see inset in Fig. 1).

The dependences of the etching rate r at the h-BN ceramics surface on the energy density F are shown in Fig. 2. For

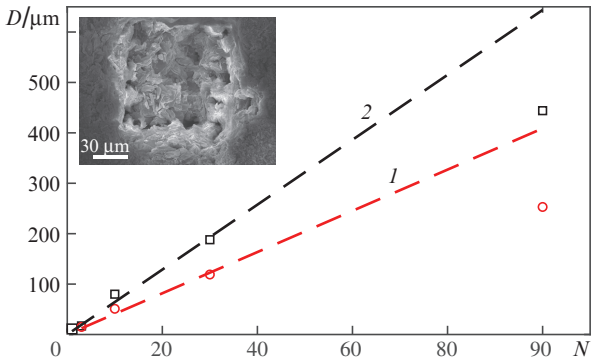

Figure 1. Dependence of the crater depth D on the number N of laser pulses at F = (*1*) 8.3 and (*2*) 18.1 J cm^{-2}. The inset shows an example of the target surface relief after laser irradiation.

both wavelengths (193 and 248 nm), the ablation curves consist of two sections, each of which is close to a logarithmic dependence: $r = L_0 \ln(F/F_{th})$, where F_{th} characterises the threshold energy at which ablation develops, and L_0 is determined by the layer thickness heated during a pulse. The first ablation regime with a heating depth of 100–200 nm and a threshold of about 0.3–0.5 J cm^{-2} (depending on the wavelength) is realised at $F < 1-2$ J cm^{-2}. At $F > 1-2$ J cm^{-2}, the second regimes is observed, characterised by a much higher value of L_0 (700–2000 nm) and, as a result, by extreme rates of material removal. A sharp increase in the roughness of the

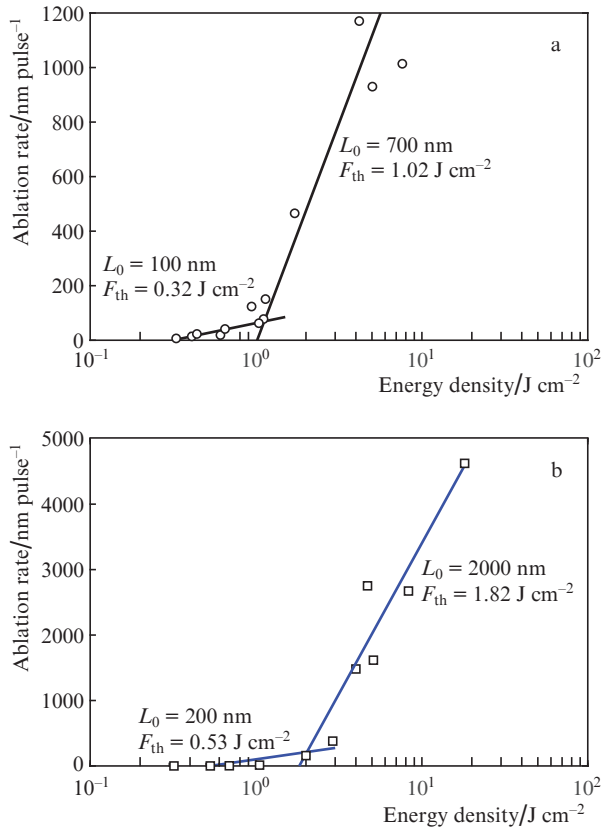

Figure 2. Ablative dependences of h-BN ceramics irradiated at wavelengths of (a) 193 and (b) 248 nm. The solid lines are the function $r \sim L_0 \ln(F/F_{th})$.

bottom and walls of the crater during the transition from the first ablation regime to the second one was not observed. The exact values of F_{th} and L_0 for each of the regimes for both wavelengths are shown in Fig. 2.

It is generally accepted that in the case of nanosecond radiation, the depth of heating of the material in the ablation zone is determined by the depth of thermal diffusion. For ceramics of hexagonal boron nitride, the thermal diffusivity coefficient χ can be estimated based on the value of the thermal conductivity coefficient taken for the h-BN crystal with crystal lattice layers perpendicular to the heat flux: k = 30 W mK^{-1}. Then, $\chi \approx 0.18$ cm^2 s^{-1}, and the depth of thermal diffusion at a time $\tau = 10$ ns is $\sqrt{\chi\tau} \approx 400$ nm, which agrees with the L_0 values measured for the first ablation regime.

Note also that the values of L_0 for different wavelengths differ by half. If we assume that the depth of radiation absorption in the target is comparable to the depth of thermal diffusion, then this difference corresponds to different optical absorption coefficients at wavelengths of 193 and 248 nm. It is difficult to assess the validity of this assumption, since the optical properties of h-BN are not fully investigated. For example, the band gap for hexagonal boron nitride varies in the literature from 3.6 to 7.1 eV [22].

The mechanism of the regime of extreme ablation rates is much less clear. Note that this behaviour of BN ceramics was observed previously. Daniel et al. [19] demonstrated a sharp increase in the ablation dependence obtained under irradiation of cubic boron nitride (c-BN) with picosecond pulses. Further research is needed to understand this ablation regime. At this stage, among the possible reasons, we will distinguish a higher thermal conductivity of the intergranular binder in ceramics, which should lead to deeper heating and enhanced ablation, starting from some certain threshold pulse energy. It is impossible to exclude the influence of the shock wave, which increases the mechanical destruction in the ablation zone, especially along the boundaries of the crystals. Finally, c-BN ceramics may be characterised by an effect of enhanced optical absorption at the microcrystal boundaries, which also contributes to the removal of the material with whole grains. Note that the above-described development of roughness at the bottom of a deep crater and the supposedly related effect of reducing the ablation rate (see Fig. 1) were observed only in the regime of extreme rates, which is consistent with the hypothesis of h-BN ceramics thermoelastic fracture along intergranular boundaries.

An important factor from the point of view of producing an X-ray refractive element is the verticality of the channel walls during plate cutting. Figure 3 shows the dependence of the slope of the ablation crater wall on the laser energy flux density. It can be seen that the slope is rather small ($\phi < 20°$) and weakly depends on the radiation intensity. At the same time, to obtain an almost vertical wall, relatively low radiation intensities are necessary. For comparison, in diamond, the slope of the crater wall is 20–30° with an energy density in the beam of about 12 J cm^{-2} (see Fig. 3). Qualitatively, this behaviour can be explained in the framework of a simple approach, which takes into account a decrease in energy flux with increasing angle of radiation incidence. In this approximation, the formed slope angle will be determined by the ratio of the laser energy density on the wall and the ablation threshold: $F\cos(90° - \phi) = F_{th}$. Figure 3 shows the corresponding curves for h-BN ceramics ($F_{th}^{BN} = 0.32$ J cm^{-2}) and diamond ($F_{th}^{diam} = 2$ J cm^{-2}), which demonstrate qualitative agreement with the experiment.

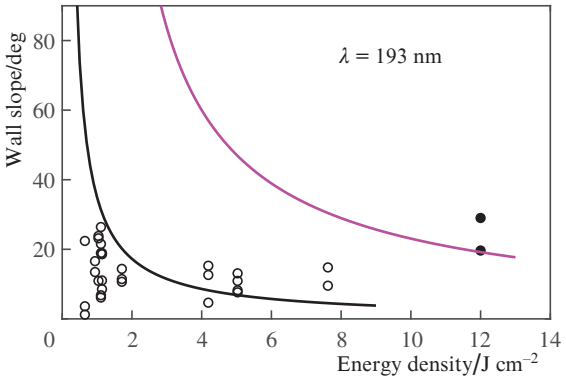

Figure 3. Dependences of the slope of the ablation crater wall on the laser energy flux density for (○) BN ceramics and (●) diamond (angle ϕ is measured from the vertical). The solid curves are the function $\sin\phi = F_{th}/F$ ($F_{th}^{BN} = 0.32$ J cm^{-2}, $F_{th}^{diam} = 2$ J cm^{-2}).

4. Conclusions

We have studied the ablation characteristics of hexagonal boron nitride ceramics irradiated by 193- and 248-nm UV laser pulses.

We have found that in both cases, the dependences of the etching rate on the energy density has two sections that characterise different mechanisms of energy penetration into the material. When the density of the laser energy is below 1–2 J cm^{-2}, the depth of heating is approximately 100–200 nm and is determined by the thermal conductivity of hexagonal boron nitride. At higher energy densities, the penetration depth is 700–2000 nm. In this case, the ablation rates of the material reach 1–5 μm per pulse, which is generally not typical of nanosecond radiation. We have also shown that due to the low ablation threshold (about 0.3–0.5 J cm^{-2}, depending on the wavelength), the crater wall formed during drilling of boron nitride at relatively low beam intensities is close to vertical ($\phi < 20°$), which opens up interesting prospects for laser processing of thick BN plates, in particular when forming the profile of X-ray elements.

Acknowledgements. This work was supported by the Ministry of Education and Science of the Russian Federation (Project No. 3.2608.2017/PCh).

References

1. Du X.Z., Li J., Lin J.Y., Jiang H.X. *Appl. Phys. Lett.*, **106**, 021110 (2015).
2. Tran T.T., Bray K., Ford M.J., Toth M., Aharonovich I. *Nature Nanotechnol.*, **11**, 37 (2016).
3. Shotan Z., Jayakumar H., Considine C.R., Mackoit M., Fedder H., Wrachtrup J., Alkauskas A., Doherty M.W., Menon V.M., Meriles C.A. *ACS Photon.*, **3**, 2490 (2016).
4. Yu D.P., Sun X.S., Lee C.S., Bello I., Lee S.T., Gu H.D., Leung K.M., Zhou G.W., Dong Z.F., Zhang Z. *Appl. Phys.Lett.*, **72**, 1966 (1998).
5. Park J.-H., Park J.C., Yun S.J., Kim H., Luong D.H., Kim S.M., Choi S.H., Yang W., Kong J., Kim K.K., Lee Y.H. *ACS Nano*, **8**, 8520 (2014).
6. Snigirev A., Kohn V., Snigireva I., Lengeler B. *Nature*, **384**, 49 (1996).
7. Lengeler B., Tümmler J., Snigirev A., Snigireva I., Raven C. *J. Appl. Phys.*, **84**, 5855 (1998).
8. Kononenko T.V., Ralchenko V.G., Ashkinazi E.E., Polikarpov M., Ershov P., Kuznetsov S., Yunkin V., Snigireva I., Konov V.I. *Appl. Phys. A*, **122**, 152 (2016).

9. Kessler G., Bauer H.D., Pompe W., Scheibe H.J. *Thin Solid Films*, **147**, L45 (1987).
10. Angleraud B., Girault C., Champeaux C., Garrelie F., Germain C., Catherinot A. *Appl. Surface Sci*., **96–98**, 117 (1996).
11. Ohba H., Saeki M., Esaka F., Yamada Y., et al. *J. Vacuum Soc. Japan*, **52** (6), 369 (2009).
12. Sokołowski M., Sokołowska A., Wronikowski M., Kosik T. *J. Mater. Sci*., **25**, 263 (1990).
13. Golberg D., Rode A., Bando Y., Mitome M., Gamaly E., Luther-Davies B. *Diamond and Related Materials*, **12**, 1269 (2003).
14. Laude T., Matsui Y., Marraud A., Jouffrey B. *Appl. Phys. Lett.*, **76**, 3239 (2000).
15. Kanaev A.V., Petitet J.-P., Museur L., Marine V., Solozhenko V.L., Zafiropulos V. *J. Appl. Phys*., **96**, 4483 (2004).
16. Museur L., Anglos D., Petitet J.-P., Michel J.-P., Kanaev A.V. *J. Luminescence*, **127**, 595 (2007).
17. Walter C., Rabiey M., Warhanek M., Jochum N., Wegener K. *CIRP Annals*, **61**, 279 (2012).
18. Sumiyoshi T., Tomita H., Takahashi A., Obara M., Ishii K. *J. Appl. Phys*., **79**, 2831 (1998).
19. Daniel C., Ostendorf S., Hallmann S., Emmelmann C. *J. Laser Appl.*, **28**, 012001 (2015).
20. Hirayama Y., Obara M. *J. Appl. Phys*., **90**, 6447 (2001).
21. Hitchcock L., Kim G.-S., Reck G., Rothe E. *J. Quantum Spectrosc. Radiat. Transfer*, **44** (3), 3730378 (1990).
22. Solozhenko V.L., Lazarenko A.G., Petitet J.P., Kanaev A.V. *J. Phys. Chem. Solids*, **62**, 1331 (2001).